NASA/TM—2003-212583

LS-DYNA Implementation of Polymer Matrix Composite Model Under High Strain Rate Impact

Xiahua Zheng
University of Akron, Akron, Ohio

Robert K. Goldberg
Glenn Research Center, Cleveland, Ohio

Wieslaw K. Binienda
University of Akron, Akron, Ohio

Gary D. Roberts
Glenn Research Center, Cleveland, Ohio

September 2003

The NASA STI Program Office . . . in Profile

Since its founding, NASA has been dedicated to the advancement of aeronautics and space science. The NASA Scientific and Technical Information (STI) Program Office plays a key part in helping NASA maintain this important role.

The NASA STI Program Office is operated by Langley Research Center, the Lead Center for NASA's scientific and technical information. The NASA STI Program Office provides access to the NASA STI Database, the largest collection of aeronautical and space science STI in the world. The Program Office is also NASA's institutional mechanism for disseminating the results of its research and development activities. These results are published by NASA in the NASA STI Report Series, which includes the following report types:

- TECHNICAL PUBLICATION. Reports of completed research or a major significant phase of research that present the results of NASA programs and include extensive data or theoretical analysis. Includes compilations of significant scientific and technical data and information deemed to be of continuing reference value. NASA's counterpart of peer-reviewed formal professional papers but has less stringent limitations on manuscript length and extent of graphic presentations.

- TECHNICAL MEMORANDUM. Scientific and technical findings that are preliminary or of specialized interest, e.g., quick release reports, working papers, and bibliographies that contain minimal annotation. Does not contain extensive analysis.

- CONTRACTOR REPORT. Scientific and technical findings by NASA-sponsored contractors and grantees.

- CONFERENCE PUBLICATION. Collected papers from scientific and technical conferences, symposia, seminars, or other meetings sponsored or cosponsored by NASA.

- SPECIAL PUBLICATION. Scientific, technical, or historical information from NASA programs, projects, and missions, often concerned with subjects having substantial public interest.

- TECHNICAL TRANSLATION. English-language translations of foreign scientific and technical material pertinent to NASA's mission.

Specialized services that complement the STI Program Office's diverse offerings include creating custom thesauri, building customized databases, organizing and publishing research results . . . even providing videos.

For more information about the NASA STI Program Office, see the following:

- Access the NASA STI Program Home Page at ***http://www.sti.nasa.gov***

- E-mail your question via the Internet to help@sti.nasa.gov

- Fax your question to the NASA Access Help Desk at 301–621–0134

- Telephone the NASA Access Help Desk at 301–621–0390

- Write to:
  NASA Access Help Desk
  NASA Center for AeroSpace Information
  7121 Standard Drive
  Hanover, MD 21076

NASA/TM—2003-212583

LS-DYNA Implementation of Polymer Matrix Composite Model Under High Strain Rate Impact

Xiahua Zheng
University of Akron, Akron, Ohio

Robert K. Goldberg
Glenn Research Center, Cleveland, Ohio

Wieslaw K. Binienda
University of Akron, Akron, Ohio

Gary D. Roberts
Glenn Research Center, Cleveland, Ohio

Prepared for the
35th International Technical Conference
sponsored by the Midwest Chapter of the Society for the
Advancement of Materials and Process Engineering
Dayton, Ohio, September 28–October 2, 2003

National Aeronautics and
Space Administration

Glenn Research Center

September 2003

The Propulsion and Power Program at
NASA Glenn Research Center sponsored this work.

Available from

NASA Center for Aerospace Information
7121 Standard Drive
Hanover, MD 21076

National Technical Information Service
5285 Port Royal Road
Springfield, VA 22100

Available electronically at http://gltrs.grc.nasa.gov

LS-DYNA IMPLEMENTATION OF POLYMER MATRIX COMPOSITE MODEL UNDER HIGH STRAIN RATE IMPACT

Xiahua Zheng
University of Akron
Department of Civil Engineering
Akron, Ohio

Robert K. Goldberg
National Aeronautics and Space Administration
Glenn Research Center
Cleveland, Ohio

Wieslaw K. Binienda
University of Akron
Department of Civil Engineering
Akron, Ohio

Gary D. Roberts
National Aeronautics and Space Administration
Glenn Research Center
Cleveland, Ohio

ABSTRACT

A recently developed constitutive model is implemented into LS-DYNA as a user defined material model (UMAT) to characterize the nonlinear strain rate dependent behavior of polymers. By utilizing this model within a micromechanics technique based on a laminate analogy, an algorithm to analyze the strain rate dependent, nonlinear deformation of a fiber reinforced polymer matrix composite is then developed as a UMAT to simulate the response of these composites under high strain rate impact. The models are designed for shell elements in order to ensure computational efficiency. Experimental and numerical stress-strain curves are compared for two representative polymers and a representative polymer matrix composite, with the analytical model predicting the experimental response reasonably well.

INTRODUCTION

In recent years, there is an increasing trend in the use of fiber-reinforced polymer composites to primary aircraft structures, such as the radome and the fan containment system of jet engines. For all of the above applications, accounting for and correctly computing the strain rate dependent mechanical properties of polymer matrix composites are a major concern.

To assist in designing composite structures subject to high strain rate impact loads, finite element simulation is a powerful tool and can even in some circumstances partially substitute for expensive experimental tests. Among the various commercial finite element codes, LS-DYNA [1] excels in large deformation transient dynamic problems and impact simulations due to the explicit time integration algorithms within the code.

LS-DYNA has a large library of material options which have been widely used in the automobile and aerospace industries. For example, Schweizerhof, et. al. [2] used LS-DYNA to conduct a crashworthiness analysis of a composite structure. Bilkhu, et. al. [3] studied the transverse impact response of composite plates using LS-DYNA as well. The material models for composite materials currently included within LS-DYNA are specifically designed for shell elements in order to improve the computational efficiency when conducting a structural analysis of large composite structures. However, the material models for composite materials currently included within LS-DYNA do not consider the effect of strain rate on the material response, which is an important feature in polymer matrix composites, especially under high strain rate impact. Recently, Yen [4] implemented a new composite failure model into LS-DYNA. This model uses an empirical equation to account for the effect of strain rate on the layer strength values within the composite failure criteria, and characterizes the progressive failure behavior. However, the effects of strain rate on the deformation response are not accounted for within this model, and the model is only applicable to solid elements.

In this study, a recently developed material model [5] is implemented into LS-DYNA as a user defined material (UMAT) designed for shell elements. In this material model, state variable constitutive equations originally developed for metals are modified in order to compute the nonlinear, strain rate dependent deformation of polymers, including the effects of hydrostatic stresses. These equations are then utilized within a strength of materials based micromechanics approach using a laminate analogy in order to predict the strain rate dependent deformation of polymer matrix composites. Experimentally obtained stress-strain curves of two representative polymers and a representative polymer matrix composite under both moderate and high strain rate conditions are used to verify the UMAT with a single element simulation. A set of failure criteria and a damage progression model are also proposed in this paper.

POLYMER CONSTITUTIVE EQUATIONS

To analyze the nonlinear, strain rate dependent deformation of the polymer matrix constituent, the Bodner-Partom viscoplastic state variable model [6], which was originally developed to analyze the viscoplastic deformation of metals above one-half of the melting temperature, has been modified [5,7]. In state variable models, a single unified strain variable is defined to represent all inelastic strains [8]. Furthermore, in the state variable approach there is no defined yield stress. Inelastic strains are assumed to be present at all values of stress, the inelastic strains are just assumed to be very small in the “elastic” range of deformation. State variables, which evolve with stress and inelastic strain, are defined to represent the average effects of the deformation mechanisms.

In the modified Bodner model used in this study, the components of the inelastic strain rate tensor, $\dot{\varepsilon}_{ij}^{I}$, are defined as a function of the deviatoric stress components S_{ij}, the second invariant of the deviatoric stress tensor J_2 and an isotropic state variable Z, which represents the resistance to molecular flow. The components of the inelastic strain rate are defined as follows

$$\dot{\varepsilon}_{ij}^{I} = 2D_0 \exp\left[-\frac{1}{2}\left(\frac{Z}{\sigma_e}\right)^{2n}\right]\left(\frac{S_{ij}}{2\sqrt{J_2}} + \alpha\delta_{ij}\right) \tag{1}$$

where D_0 and n are both material constants, with D_0 representing the maximum inelastic strain rate and n controlling the rate dependence of the material. The effective stress, σ_e, is defined as

$$\sigma_e = \sqrt{3J_2} + \sqrt{3}\alpha\sigma_{kk} \tag{2}$$

where α is a state variable controlling the level of the hydrostatic stress effects and σ_{kk} is the summation of the normal stress components which equals three times the mean stress.

The rate of evolution of the internal stress state variable Z and the hydrostatic stress effect state variable α are defined by the equations

$$\dot{Z} = q(Z_1 - Z)\dot{e}_e^I \tag{3}$$

$$\dot{\alpha} = q(\alpha_1 - \alpha)\dot{e}_e^I \tag{4}$$

where q is a material constant representing the "hardening" rate, and Z_1 and α_1 are material constants representing the maximum value of Z and α, respectively. The initial values of Z and α are defined by the material constants Z_0 and α_0. The term $\dot{e}_e^I$ in Equations 3 and 4 represents the effective deviatoric inelastic strain rate, which is defined as

$$\begin{aligned} \dot{e}_e^I &= \sqrt{\frac{2}{3}\dot{e}_{ij}^I\dot{e}_{ij}^I} \\ \dot{e}_{ij}^I &= \dot{\varepsilon}_{ij}^I - \dot{\varepsilon}_m^I\delta_{ij} \end{aligned} \tag{5}$$

where $\dot{\varepsilon}_{ij}^I$ are the components of the inelastic strain rate tensor and $\dot{\varepsilon}_m^I$ is the mean inelastic strain rate. In many state variable constitutive models developed to analyze the behavior of metals [8], the total inelastic strain and strain rate are used in the evolution laws and are assumed to be equal to their deviatoric values. As discussed by Li and Pan [9], since hydrostatic stresses contribute to the inelastic strains in polymers, indicating volumetric effects are present, the mean inelastic strain rate cannot be assumed to be zero, as is the case in the inelastic analysis of metals. Further information on the constitutive model, along with the procedures required to obtain the material constants, can be found in Goldberg, et al [5, 7].

COMPOSITE MICROMECHANICAL MODELING

To compute the effective strain rate dependent, nonlinear deformation response of polymer matrix composites based on the response of the individual constituents, a micromechanical model has been developed [10]. In this model, the unit cell is defined to consist of a single fiber and its surrounding matrix. Due to symmetry, only one-quarter of the unit cell is analyzed. The composites are assumed to have a periodic, square fiber packing with a perfect interfacial bond. The fibers are assumed to be transversely isotropic and linear elastic with a circular cross-section. The matrix is assumed to be isotropic, with a rate dependent, nonlinear deformation response computed using the equations described in the previous section of this report.

The unit cell is divided up into an arbitrary number of rectangular, horizontal slices, as is shown in Figure 1. Each slice is assumed to be in a state of plane stress and classical laminate theory is assumed to be applicable at this scale. The top and bottom slices in the unit cell are composed of pure matrix. The remaining slices are composed of two subslices; one composed of fiber material and the other composed of matrix material. For the slices containing both fiber and matrix, the out-of-plane stresses can be nonzero in individual subslices, but the volume average of the out-of-plane stresses must be equal to zero. By using this approach, the behavior of each slice is decoupled, and the response of each slice can be determined independently, which significantly reduces the level of complexity in the analysis. Laminate theory is used to obtain the effective response of the unit cell.

The thickness, fiber volume ratio and thickness ratio (the ratio of the slice thickness to the total unit cell thickness) for each slice can be determined using the composite fiber volume ratio and geometric principles. The overall diameter of the fiber is related to the fiber volume fraction of the overall composite, and this term can be used along with the standard geometric definition of the radius of a circle to compute the horizontal coordinate of any point on the outer surface of the fiber in terms of the fiber volume fraction and the vertical coordinate. Using this information and standard calculus concepts, the area of the portion of the fiber contained within each slice of the one-quarter of the unit cell which is analyzed can be computed. The fiber diameter and fiber area within each slice can be used to compute the fiber volume fraction and thickness ratio of each slice.

The effective properties, effective stresses and effective inelastic strains of each slice are computed independently. Micromechanics equations are developed using uniform stress and uniform strain assumptions for those slices composed of both fiber and matrix material. The stresses and inelastic strains in the slices composed of pure matrix are computed using the matrix elastic properties and the inelastic constitutive equations. The standard transversely isotropic compliance matrix (or isotropic in the case of the matrix) is used to relate the local strains to the local stresses in the fiber and matrix. Each slice is assumed to be in a state of plane stress on the global level, but out-of-plane normal stresses can exist in each subslice. The responses of each slice are combined using laminate theory to obtain the effective response of the corresponding lamina. Laminate theory is applied once again to obtain the effective properties and force resultants due to inelastic strains for a multilayered composite laminate.

DAMAGE MODEL

Fiber reinforced composites have a variety of damage mechanisms. At the micro-level, these mechanisms can include fiber fracture, fiber buckling, fiber splitting, fiber pullout, fiber/matrix debonding and matrix cracking. At the laminate level the damage mechanisms can include transverse cracks in planes parallel and perpendicular to the fibers and delamination between layers of the laminate [11].

Among the various damage modes, Langlie and Cheng [12] stated that fiber breakage, through-thickness compressive and shear punching failure and delamination are the major damage mechanisms in high strain rate impact. In a high strain rate impact environment, one can argue that a strain controlled failure model is more realistic than a stress controlled failure model. Therefore, the failure criteria for this study are defined as follows:

Fiber breakage:

$$f_1 = \frac{\varepsilon_{11}}{\varepsilon_{f11}} \geq 1 \tag{6}$$

Compressive punching failure:

$$f_2 = \frac{\varepsilon_{33}}{\varepsilon_{f33}} \geq 1 \tag{7}$$

Shear punching failure:

$$f_3 = \frac{\varepsilon_{23}}{\varepsilon_{f23}} + \frac{\varepsilon_{13}}{\varepsilon_{f13}} \geq 1 \tag{8}$$

where ε_{f11} is the fiber direction composite tensile failure strain, and ε_{f33} is the through thickness compressive composite failure strain. ε_{f23} and ε_{f13} are the through thickness shear composite failure strains. The failure mode of delamination is not included in this material model.

Once failure has occurred, two strategies can be applied to describe the post-failure behavior of the material. One option is to assume that the material fails instantaneously, while the other option is to apply a post-failure model [13]. For the instantaneous failure model, when fiber breakage occurs in the 1 direction, all stresses related to that direction (σ_{ij}, i =1, j=1−3) are set to zero instantaneously. When either compressive or shear punching failure occurs, all stresses are instantaneously set to zero.

A post-failure model based on continuum damage mechanics was reported by Matzenmiller, et. al. [14]. Recent studies conducted using this model show significant improvement in the

prediction of damage [13], [4]. This damage model characterizes the growth of damage by a decrease in the stiffness of the material. When fiber breakage occurs in the 1 direction, stiffness values in that direction and in all shear directions are reduced. When either compressive or shear punching failure occurs, all stiffness values are reduced. It can be described by the following equations:

$$S = \begin{bmatrix} \frac{1}{(1-\varpi_1)E_1} & -\frac{\nu_{21}}{E_2} & -\frac{\nu_{31}}{E_3} & 0 & 0 & 0 \\ -\frac{\nu_{12}}{E_1} & \frac{1}{(1-\varpi_2)E_2} & -\frac{\nu_{32}}{E_3} & 0 & 0 & 0 \\ -\frac{\nu_{13}}{E_1} & -\frac{\nu_{23}}{E_2} & \frac{1}{(1-\varpi_3)E_3} & 0 & 0 & 0 \\ 0 & 0 & 0 & \frac{1}{(1-\varpi_4)G_{12}} & 0 & 0 \\ 0 & 0 & 0 & 0 & \frac{1}{(1-\varpi_5)G_{23}} & 0 \\ 0 & 0 & 0 & 0 & 0 & \frac{1}{(1-\varpi_6)G_{31}} \end{bmatrix} \quad (9)$$

where S is the compliance matrix, and the stiffness matrix C is obtained by inverting S, that is $[C] = [S]^{-1}$

ϖ_i is the damage variable associated with the i^{th} failure mode to relate the onset and growth of damage to stiffness losses in the material, which can be obtained from an individual failure mode j as

$$\varpi_i = 1 - e^{\frac{1}{m}\left(1 - f_j^m\right)} \quad (10)$$

where m is the damage exponent, and f_j (j=1−3) is the damage parameter as described in equations (6)-(8). At the onset of failure, the value of ϖ_i is zero. As damage progresses, ϖ_i increases and therefore eventually decreases the stiffness of the material until it reaches a final value of zero.

LS-DYNA IMPLEMENTATION AND MODEL VERIFICATION

LS-DYNA has a user defined material option where a user can implement his or her own material model into the code through the use of a UMAT subroutine. The structure of the subroutine is shown in the Figure 2. The LS-DYNA code calculates the strain increments for a time step and passes them to the UMAT subroutine at the beginning of each time step. The material constants, such as moduli and Poisson's ratios, are read from the LS-DYNA input file by the subroutine. The current value of the state variables such as Z and α are saved as history

variables which can be read in by the subroutine. By using the history variables, material constants and strain increments, the subroutine is able to calculate the stresses at the end of the time step by using an incremental form of the polymer constitutive equations and the composite micromechanics equations. The subroutine then updates and saves the history variables for use in the next time step, and outputs the calculated stresses together with the through thickness strain increment. For shell elements under plane stress conditions, the through thickness strain increment for the time step must be computed in the UMAT subroutine. The subroutine also checks the damage and modifies the material stiffness if damage occurs. The procedure described above is carried out on each integration point of each element independently.

As a first step in implementing the analytical model into LS-DYNA, the polymer constitutive model was implemented into the code as a UMAT. To verify the analytical model and its implementation within LS-DYNA, two representative toughened epoxies, PR520 and 977-2, were analyzed using LS-DYNA, and the computed stress-strain curves were compared to experimental results obtained by Goldberg, et. al. [5, 7]. In the experimental tests, longitudinal tensile tests and pure shear tests were conducted at room temperature on the materials at strain rates of about $5x10^{-5}$ /sec, 1 /sec and 400 /sec. The low and moderate strain rate tests were conducted using an Instron hydraulic testing machine. The high strain rate tests were conducted using a split Hopkinson bar. Engineering stress and engineering strain were measured until failure.

In the finite element analyses, a four-node single Belytschko-Tsay shell element was used for the simulation of the pure shear and tension tests. The load and boundary conditions applied to the model are shown in Figure 3. The applied strain rate is controlled by the displacement-time curve defined in the LS-DYNA input file. Since LS-DYNA is an explicit code, designed for solving dynamic problems, attempts to simulate the extremely low stain rate tests were found to have numerical stability problems, and the analyses took an extremely long time to reach the failure strain, even by using only a single element. In addition, in a realistic impact problem, the strain rates are well above the quasi-static level. Therefore, the low strain rate case of $5x10^{-5}$ /sec was not considered here. Table 1 lists the material constants used in the model, which were determined using the procedures described in Goldberg, et. al. [5, 7].

TABLE 1.—MATERIAL CONSTANTS USED IN POLYMER MATRIX MODELING

	Strain Rate (1/sec)	Modulus (GPa)	Poisson's Ratio	D_o (1/sec)	n	Z_o (MPa)	Z_1 (MPa)	q	α_o	α_1
PR520	1.76	3.54	0.38	$1x10^6$	0.93	396.09	753.82	279.26	0.568	0.126
	420	7.18								
977-2	1.9	3.52	0.40	$1x10^6$	0.85	259.50	1131.4	150.50	0.129	0.152
	500	6.33								

Experimental [5,7] and computed shear stress-shear strain curves for PR520 are shown in Figure 4 for the moderate and high strain rate cases, while tensile stress-strain curves are shown in Figure 5. Experimental [5] and computed shear stress-shear strain curves for 977-2 are shown in

Figure 6, and tensile stress-strain curves are shown in Figure 7. Both materials exhibit a strain rate dependent, nonlinear deformation response under both shear and tensile loading. For the experimental data, at high strain rates, the sharp increase in stress at the beginning of the loading with negligible increase in strain observed for PR520 under shear and tensile loading is most likely not representative of the actual material behavior, but rather an artifact of the experimental tests. Also note that the oscillations observed in the high strain rate tensile tests for 977-2 were a result of the specimen geometry that was utilized for these tests.

From Figures 4-7, it can be seen that the finite element results under shear loading correlate reasonably well with the experimental data for both materials. The nonlinearity and rate dependence observed in the deformation of the two polymers are captured qualitatively, and the quantitative match between the experimental and computed results is reasonably good. For the tensile loading condition, while the strain rate dependence and nonlinearity of the stress-strain results are correctly captured qualitatively, for the PR520 material at the moderate strain rate the stresses in the nonlinear portion of the stress-strain curve are under predicted for reasons that require further investigation. One possible cause for the discrepancy may be that the beginning and final values of the hydrostatic stress state variable α (α_0 and α_1) actually vary with strain rate, while in this study these values were assumed to be constant and were determined using low strain rate data not included here. For the PR520 material under high strain rate tensile loading, the slope of the nonlinear portion of the stress-strain curve matches the slope of the experimental curve, and if the experimental curve was shifted appropriately the comparison between the experimental and computed results may actually be quite good. For the 977-2 material under tensile loading, at the moderate strain rate in the nonlinear portion of the stress-strain curve the stresses are still slightly under predicted, but the comparison between the experimental and computed results are much improved as compared to the PR520 predictions. For 977-2 under high strain rate tensile loading, the predicted stress-strain curve bisects the experimental curve, indicating that the predictions may adequately represent the actual material behavior.

The next step in the analysis process involved implementing the composite micromechanical model into LS-DYNA through the use of a UMAT user defined subroutine. A series of analysis studies were then carried out to verify the finite element implementation of this model.

The composite material used for the verification studies consists of carbon IM7 fibers in the 977-2 toughened epoxy matrix discussed earlier. Each composite was defined to have four plies with a fiber volume of 0.60. The properties for 977-2 matrix are the same as defined in Table 1. The IM7 fiber properties are as follows: E_{11}=276 GPa, E_{22}=13.8 GPa, ν_{12}=0.25, ν_{23}=0.25, G_{12}=20.0 GPa. The loading and boundary conditions used for the composite verification studies are identical to those used for the verification studies for the polymer constitutive equations.

Experimental [5] and predicted longitudinal tensile stress-strain curves for two laminate configurations ([45°] and [90°]) of the IM7/977-2 material at strain rates of approximately 1 /sec and 400 /sec are shown in Figure 8 and Figure 9. In Figure 8, for the [45°] laminate at the high strain rate the LS-DYNA stress-strain curve exhibited a wave shape, which may due to the shock wave from the boundary induced by the high strain rate load on the single element. This discrepancy will be investigated further. In Figure 9, the experimental curve shows a higher stress at the initial stage of loading than the numerical results. However, the high stress levels

seen in the experimental curves may be an artifact of the way the stress waves progress through the specimen at the start of the experiment, and the computations may actually be fairly accurate. At higher strain levels, the comparison is much improved. The comparison between the experimental and numerical results is excellent for the moderate strain rate in both of the laminate configurations.

A preliminary attempt to exercise the damage models is shown in Figure 10 for the progressive damage model. The bulk polymer PR520 was analyzed under tensile loading at the moderate strain rate of 1.4 /sec. It can be seen that by adjusting the damage exponent *m*, damage progression can be controlled. Large values of m represent brittle fracture, whereas lowering the value of *m* increases the post-failure strength.

CONCLUSIONS

State variable constitutive equations based on the Bodner viscoplasticity model have been modified to analyze the nonlinear, strain rate dependent deformation of polymers. The effects of hydrostatic stresses on the inelastic deformation have been accounted for. The constitutive equations have been implemented within the LS-DYNA transient dynamic finite element code through the use of user defined subroutines (UMATs). The tensile and shear deformation of two representative polymers have been accurately simulated using the polymer UMAT with the constitutive model.

The polymer constitutive equations were then implemented into a composite micromechanical model where the unit cell has been divided into several independently analyzed slices. The composite model has also been implemented into LS-DYNA through the use of a UMAT. The tensile deformation of a representative polymer matrix composite was successfully predicted for two fiber orientations and two strain rates, indicating that the composite UMAT is able to capture the important features of the deformation response. There were some discrepancies between the experimental and predicted responses when high strain rate tests were simulated. The causes of these discrepancies will be investigated further.

A set of damage criteria and a damage progression model was also proposed in this paper. The damage progression model was implemented into the polymer UMAT as an initial attempt to develop a damage model for the entire composite. Once the damage model is developed to the point where it can be applied to the constituents of the composite, the damage model has great potential to predict and simulate the composite damage progression. Therefore, the damage progression model will be further developed and implemented into the composite UMAT.

The current composite UMAT is based on a plane stress assumption. Future work will incorporate the out-of-plane transverse shear stresses in order to more accurately predict the material deformation under impact conditions. Since the composite UMAT is based on micromechanics, the model will be modified to allow for the analysis of woven and braided composites.

REFERENCES

1. LS-DYNA Keyword User's Manual Version 940, Livermore Software Technology Corporation, Livermore, CA, 1997.
2. K. Schweizerhof, K. Weimar, Th. Münz. and Th. Rottner, "Crashworthiness analysis with enhanced composite material models in LS-DYNA- Merits and limits", Proceedings of the 5th international LS-DYNA users conference, Southfield, MI, 1998.
3. S.S. Bilkhu, M. Founas, W. Fong and V. Agaram, "Dynamic response of CSM composite plates—simulation using material #58 in LS-DYNA3D", Proceedings of the 9th Advanced Composites Conference, Detroit, MI, 1997.
4. C.F. Yen, "Ballistic impact modeling of composite materials", Proceedings of the 7th international LS-DYNA users conference, Detroit, MI, 2002.
5. R.K. Goldberg, G.D. Roberts and A. Gilat, "Implementation of an Associative Flow Rule Including Hydrostatic Stress Effects into the High Strain Rate Deformation Analysis of Polymer Matrix Composites", NASA/TM—2003-212382, National Aeronautics and Space Administration, June 2003.
6. S.R. Bodner, Unified plasticity for engineering applications, Kluwer Academic/Plenum Publishers, New York, 2002.
7. R.K. Goldberg, G.D. Roberts and A. Gilat, "Incorporation of Mean Stress Effects into the Micromechanical Analysis of the High Strain Rate Response of Polymer Matrix Composites", Composites Part B, **34**, pp. 151-165 (2003).
8. D.C. Stouffer and L.T. Dame, Inelastic Deformation of Metals, Models, Mechanical Properties and Metallurgy, John Wiley and Sons, New York, 1996.
9. F.Z. Li and J. Pan, "Plane-stress crack-tip fields for pressure-sensitive dilatant materials", Journal of Applied Mechanics, **57**, pp.40-49, (1990).
10. R.K. Goldberg, "Implementation of Fiber Substructuring Into Strain Rate Dependent Micromechanics Analysis of Polymer Matrix Composites", NASA/TM-2001—210822, National Aeronautics and Space Administration, April 2001.
11. C.T. Herakovich, Mechanics of Fibrous Composites, John Wiley and Sons, 1998, pp.303.
12. S. Langlie and W. Cheng, "A high velocity penetration model for thick fiber-reinforced composites", ASME Pressure vessels and piping division, **174**, 1989, pp.151-158.
13. J. Van Hoof, M.J. Woeswick, P.V. Straznicky, M. Bolduc and S. Tylko, Proceedings of the 5th international LS-DYNA users conference, 1998.
14. Matzenmiller, J. Lubliner and R.L. Taylor, "A constitutive model for anisotropic damage in fiber-composites", Mechanics of materials, **20**, 1995, pp. 125-152.

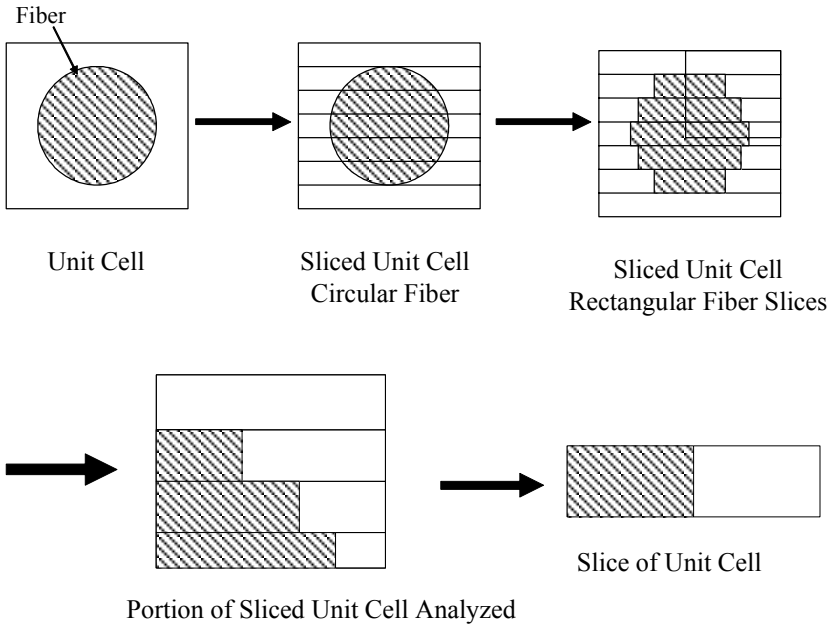

Figure 1.—Unit cell and slices in the micromechanical model

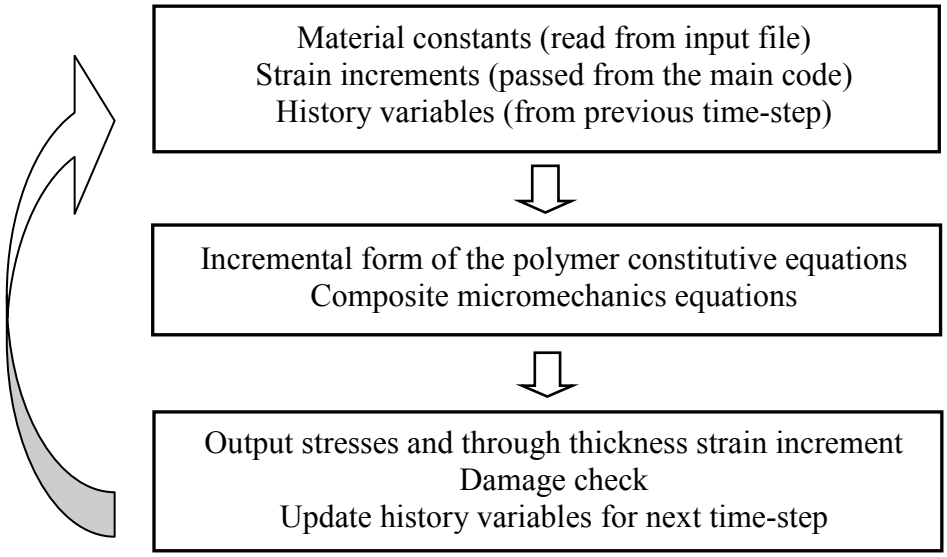

Figure 2.—Flowchart of user defined subroutine used to implement material model within LS-DYNA finite element code.

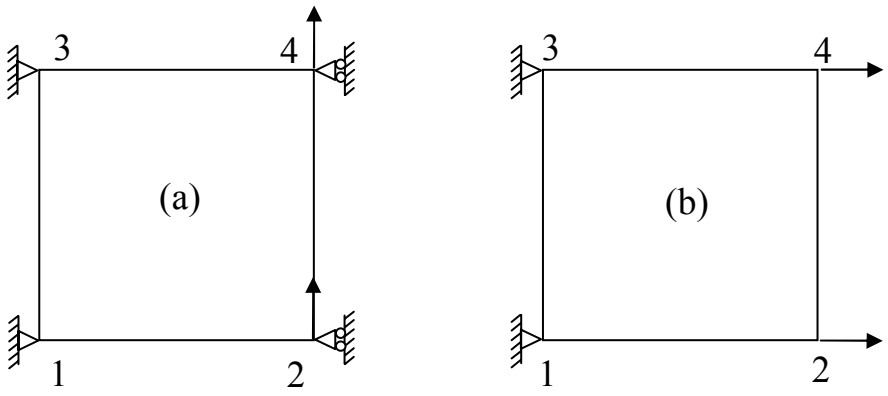

Figure 3.—Boundary and loading conditions for single element
(a) shear and (b) tension finite element analyses

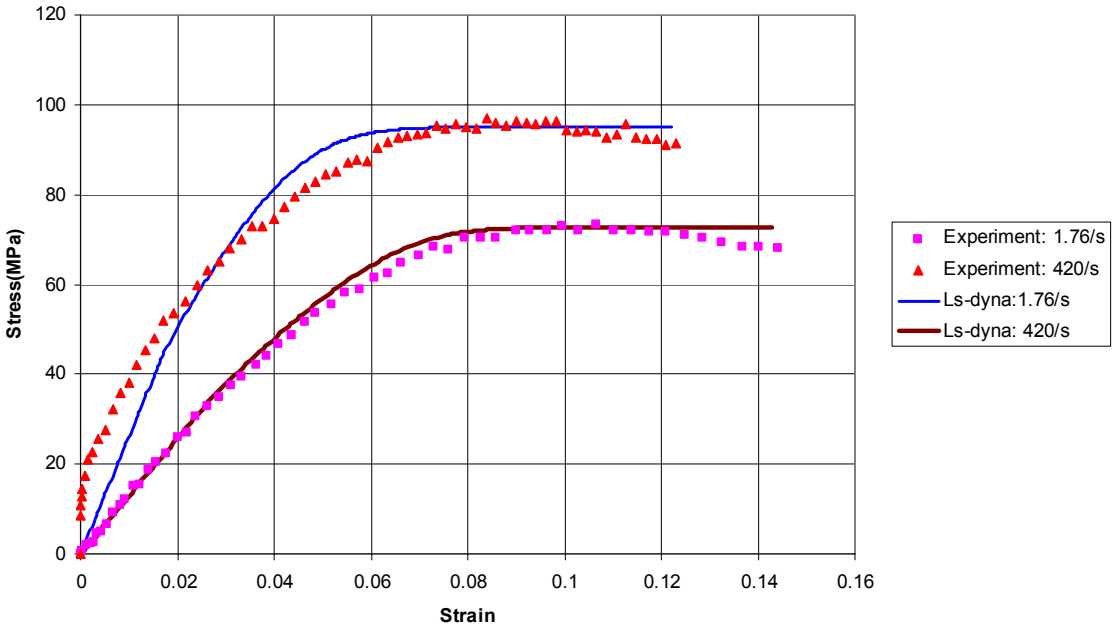

Figure 4.—Experimental and LS-DYNA simulated shear stress-shear strain curves
for PR520 resin at strain rates of 1.76 /sec and 420 /sec

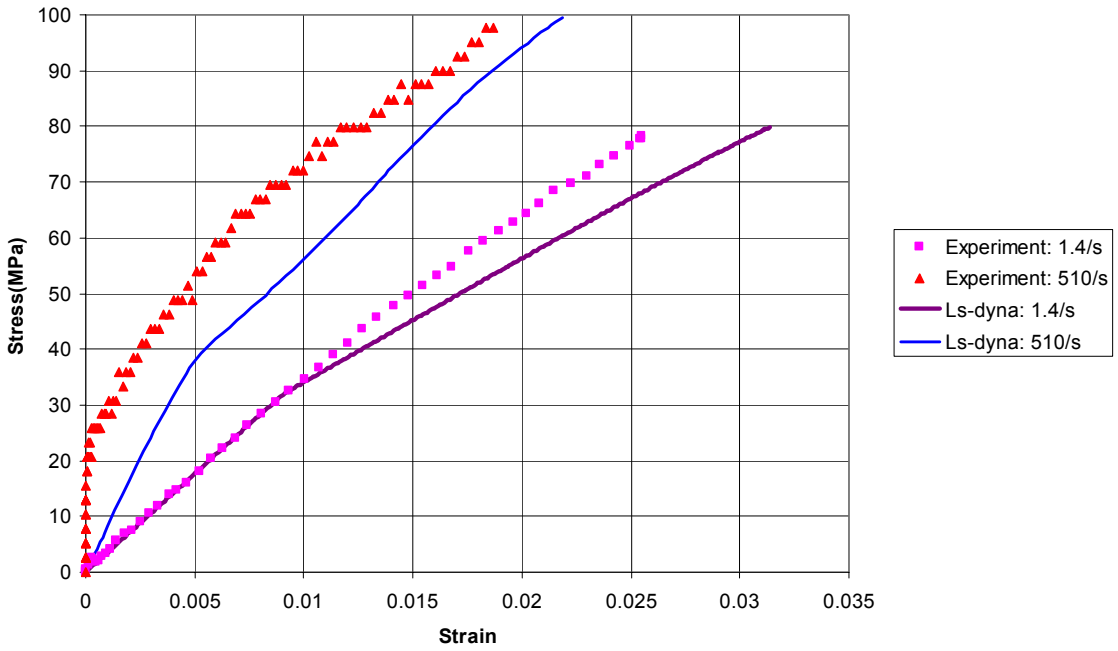

Figure 5.—Experimental and LS-DYNA simulated tensile stress-strain curves for PR520 resin at strain rates of 1.4 /sec and 510 /sec

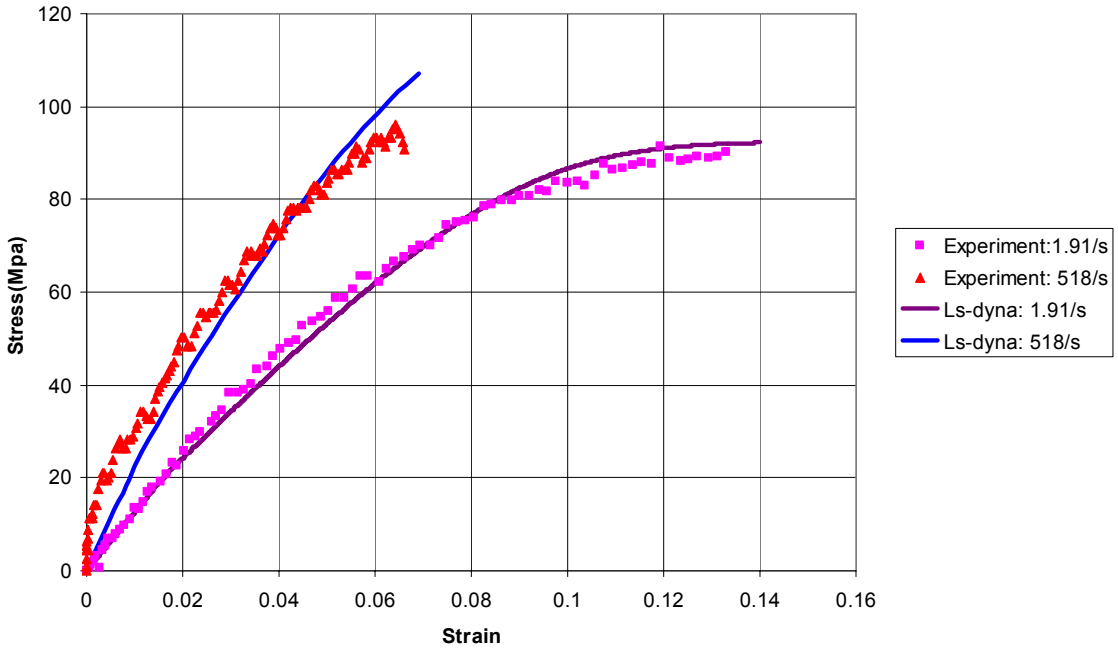

Figure 6.—Experimental and LS-DYNA simulated shear stress-shear strain curves for 977-2 resin at strain rates of 1.91 /sec and 518 /sec

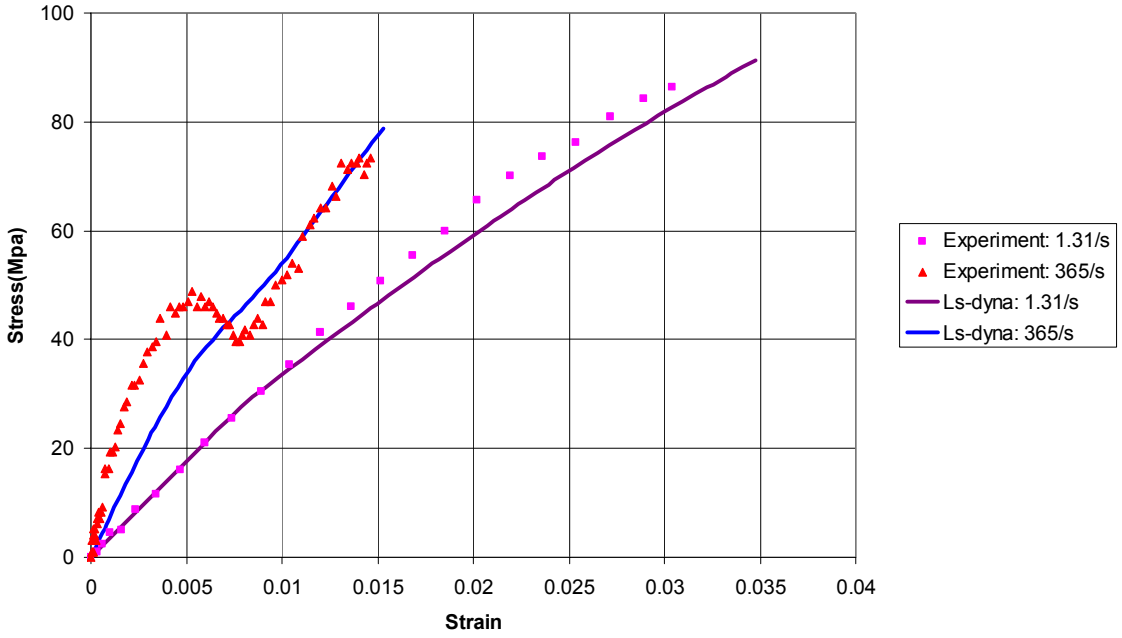

Figure 7.—Experimental and LS-DYNA simulated tensile stress-strain curves for 977-2 resin at strain rates of 1.31 /sec and 365 /sec

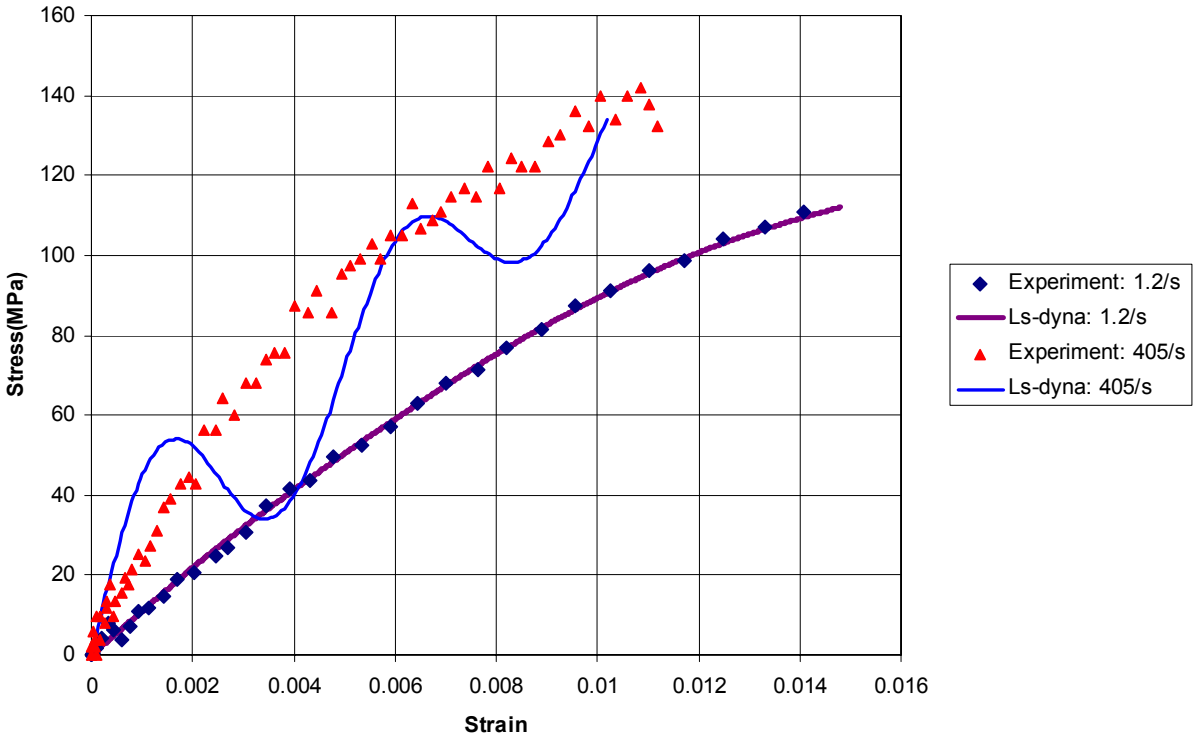

Figure 8.—Experimental and LS-DYNA simulated tensile stress-strain curves for IM7/977-2 [45°] composite at strain rates of 1.2 /sec and 405 /sec.

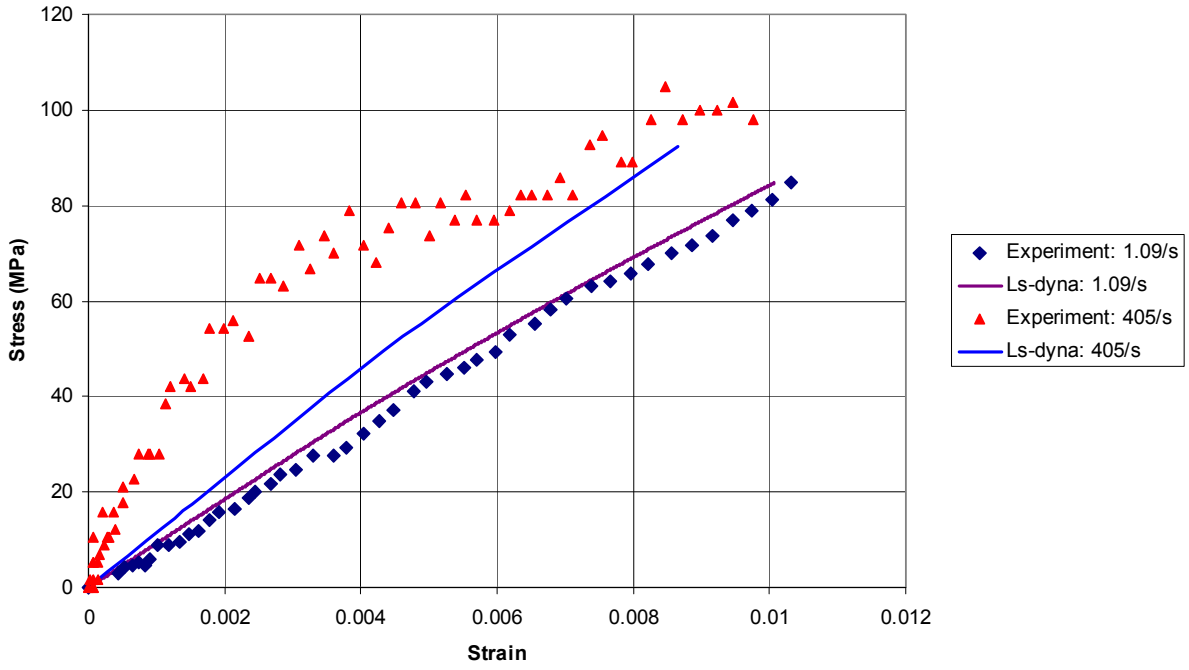

Figure 9.—Experimental and LS-DYNA simulated tensile stress-strain curves for IM7/977-2 [90°] composite at strain rates of 1.09 /sec and 405 /sec.

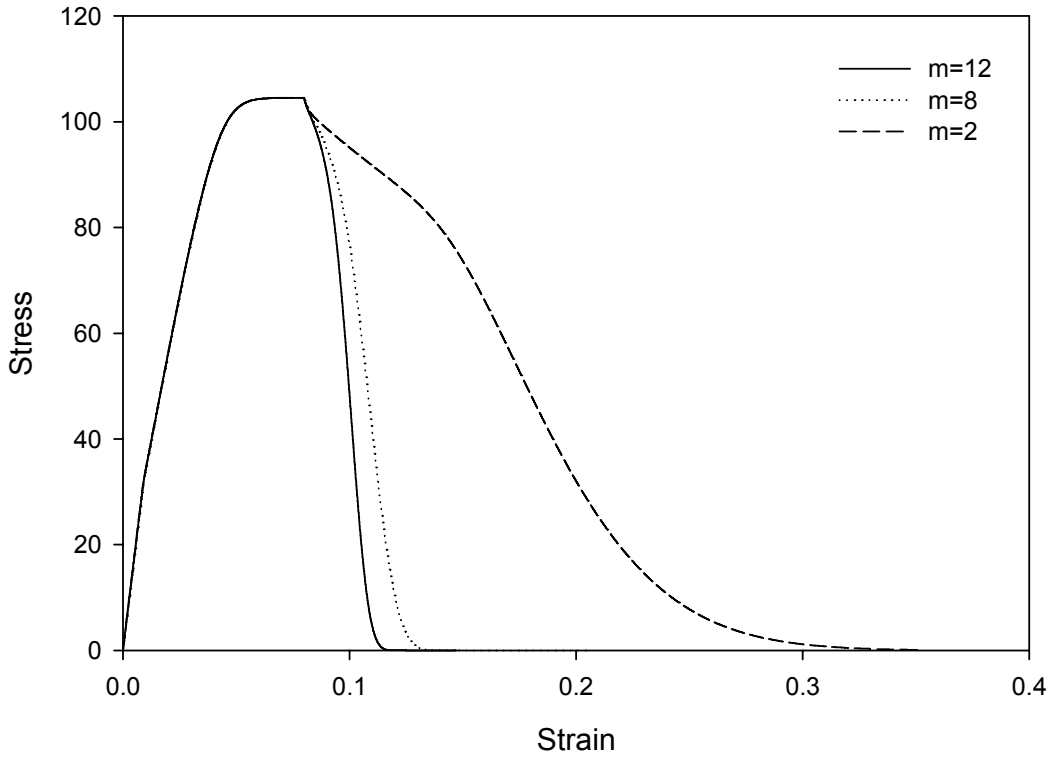

Figure 10.—Examination of the effects of damage exponent *m* on the damage progression for PR520 resin under tensile loading at a strain rate of 1.4 /sec.

REPORT DOCUMENTATION PAGE

Form Approved
OMB No. 0704-0188

1. AGENCY USE ONLY (*Leave blank*)	2. REPORT DATE	3. REPORT TYPE AND DATES COVERED
	September 2003	Technical Memorandum

4. TITLE AND SUBTITLE

LS-DYNA Implementation of Polymer Matrix Composite Model Under High Strain Rate Impact

5. FUNDING NUMBERS

WBS–22–708–24–05

6. AUTHOR(S)

Xiahua Zheng, Robert K. Goldberg, Wieslaw K. Binienda, and Gary D. Roberts

7. PERFORMING ORGANIZATION NAME(S) AND ADDRESS(ES)

National Aeronautics and Space Administration
John H. Glenn Research Center at Lewis Field
Cleveland, Ohio 44135–3191

8. PERFORMING ORGANIZATION REPORT NUMBER

E–14123

9. SPONSORING/MONITORING AGENCY NAME(S) AND ADDRESS(ES)

National Aeronautics and Space Administration
Washington, DC 20546–0001

10. SPONSORING/MONITORING AGENCY REPORT NUMBER

NASA TM—2003-212583

11. SUPPLEMENTARY NOTES

Prepared for the 35th International Technical Conference sponsored by the Midwest Chapter of the Society for the Advancement of Materials and Process Engineering, Dayton, Ohio, September 28–October 2, 2003. Xiahua Zheng and Wieslaw K. Binienda, University of Akron, Department of Civil Engineering, Akron, Ohio 44325; Robert K. Goldberg and Gary D. Roberts, NASA Glenn Research Center. Responsible person, Robert K. Goldberg, organization code 5920, 216–433–3330.

12a. DISTRIBUTION/AVAILABILITY STATEMENT

Unclassified - Unlimited
Subject Category: 24 Distribution: Nonstandard

Available electronically at http://gltrs.grc.nasa.gov

This publication is available from the NASA Center for AeroSpace Information, 301–621–0390.

12b. DISTRIBUTION CODE

13. ABSTRACT ***(Maximum 200 words)***

A recently developed constitutive model is implemented into LS-DYNA as a user defined material model (UMAT) to characterize the nonlinear strain rate dependent behavior of polymers. By utilizing this model within a micromechanics technique based on a laminate analogy, an algorithm to analyze the strain rate dependent, nonlinear deformation of a fiber reinforced polymer matrix composite is then developed as a UMAT to simulate the response of these composites under high strain rate impact. The models are designed for shell elements in order to ensure computational efficiency. Experimental and numerical stress-strain curves are compared for two representative polymers and a representative polymer matrix composite, with the analytical model predicting the experimental response reasonably well.

14. SUBJECT TERMS

Polymer matrix composites; Constitutive equations; Strain rate; Impact; Micromechanics; Finite element analysis; Composite materials; Impact analysis

15. NUMBER OF PAGES

21

16. PRICE CODE

17. SECURITY CLASSIFICATION OF REPORT	18. SECURITY CLASSIFICATION OF THIS PAGE	19. SECURITY CLASSIFICATION OF ABSTRACT	20. LIMITATION OF ABSTRACT
Unclassified	Unclassified	Unclassified	